



**AN EMPIRICAL APPROACH TO SIMULATE
THE CONCRETE SOFTENING MECHANISM**

A MASTER THESIS
SUBMITTED TO THE SCHOOL OF CIVIL, ENVIRONMENTAL
AND MINING ENGINEERING
UNIVERSITY OF ADELAIDE
FOR THE DEGREE OF
MASTER OF ENGINEERING SCIENCE

By
RATNI NURWIDAYATI

October 2011

ABSTRACT

Material properties of concrete play an important role in the analysis of reinforced concrete RC members. One of the most commonly used material properties is the compressive stress strain σ - ε relationship. Uniaxial compression tests on concrete cylinders are used to obtain these material properties of concrete in compression. These tests are effective up to peak stress, but have limited applicability post-peak stress, primarily due to the influence of size. These cause the absence of an accurate material softening stress-strain relationship. Hence, the post-peak softening behavior of a reinforced concrete member is not been able to be simulated accurately since there is not an accurate softening σ - ε relationship for concrete. An alternative approach is required.

Recently, shear friction theory has been used to simulate the softening behavior of concrete. Shear friction theory quantifies the relationship between the shear stress, normal stress, displacement and separation of the softening concrete in relation to the adjacent (non softening) concrete. In this thesis, an approach is presented to extract the shear-friction softening properties of concrete from experimental tests on long concrete prisms. Empirical mathematical expressions are developed which quantify the relationship between the softening stress and the displacement of the softening wedge. These empirical stress-displacement expressions are then applied to the analysis of eccentrically loaded concrete prisms. The theoretical analyses of these eccentrically loaded prisms agree well with the experimental results, indicating the applicability of using this approach to extract the softening shear-friction properties of concrete, from prism tests, and subsequently using these empirical expressions to simulate the post peak response of concrete.

STATEMENT ORIGINALITY

I, Ratni Nurwidayati certify that this work contains no material which has been accepted for the award of any other degree or diploma in any university or other tertiary institution and, to the best of my knowledge and belief, contains no material previously published or written by another person, except where due reference has been made in the text.

I give consent to this copy of my thesis, when deposited in the University Library, being available for loan and photocopying, subject to the provisions of the Copyright Act 1968.

I also give permission for the digital version of my thesis to be made available on the web, via the University's digital research repository, the Library catalogue and also through web search engines, unless permission has been granted by the University to restrict access for a period of time.

Ratni Nurwidayati

Date

LIST OF PUBLICATION

The following journal paper was written based on the work presented in this thesis.

Nurwidayati, R., Haskett, M., Oehlers, D. J., and Wu, C. (2011). “Wedge based concrete compression failure in RC members.” Submitted to Materials and Structures.

PUBLICATION

Wedge based concrete compression failure in RC members

¹Ratni Nurwidayati, ²Matthew Haskett, ³Deric J. Oehlers and ⁴Chengqing Wu

Mrs. Ratni Nurwidayati

¹Masters student

School of Civil, Environmental and Mining Engineering

University of Adelaide

South Australia 5005

AUSTRALIA

Corresponding author:

²Dr. Matthew Haskett

Research Associate

School of Civil, Environmental and Mining Engineering

University of Adelaide

South Australia 5005

AUSTRALIA

email: mhaskett@civeng.adelaide.edu.au

Tel. +61 8 8303 3710

Fax. +61 8 8303 4359

³Professor Deric J. Oehlers

School of Civil, Environmental and Mining Engineering

University of Adelaide

South Australia 5005

AUSTRALIA

⁴Dr. Chengqing Wu

Senior Lecturer,

School of Civil, Environmental and Mining Engineering

University of Adelaide

South Australia 5005

AUSTRALIA

1/7/11

Submitted to Materials and Structures

Wedge based concrete compression failure in RC members

R. Nurwidayati · M. Haskett · D. J. Oehlers · C. Wu

Abstract It is generally accepted that the ductility of a reinforced concrete member is a very important parameter as it governs such things as moment redistribution, moment magnification and the ability to absorb energy. Quantifying the ductility of RC members has been an almost intractable problem for a number of reasons, one of which is that it is difficult to replicate the behaviour of the compression wedge that is formed when concrete softens. A common approach used to quantify the ductility is to use concrete softening stress-strain relationships in conjunction with hinge lengths both of which have to be derived empirically. However these softening stress-strain relationships, that are derived from cylinder tests, have been found to be both size and shape dependent and it has been even more difficult to find empirically derived hinge lengths that are generic. An alternative approach is described in this paper in which the behaviour of the compression wedges are measured directly from simple tests on uniaxially loaded prisms of varying dimensions. It is shown how these prism tests in which there is a uniform strain can be used in the analysis of the compression zone of flexural members in which there is a strain gradient and without the need for hinge lengths. It is suggested that this may be a useful approach in developing new concrete products such as very high strength concrete or fibre concrete, as the effect of the new concrete product on the ductility of flexural members of any cross-sectional properties can be ascertained through a relatively few simple experimental prism tests.

Keywords Reinforced concrete · Reinforced concrete ductility · Concrete · Concrete softening

1. Introduction

Tests of reinforced concrete members clearly shows that failure of the concrete in compression, that is the softening of concrete, is associated with the formation of compression wedges [1-3] as in Fig. 1 and researchers have studied this directly through tests on eccentrically loaded prisms [4,5]. However, it is common in research practice not to quantify concrete compressive failure directly through measuring the behaviour of the wedge, but indirectly through the stress-strain relationships from compressive cylinder tests whilst softening [6,7,8]. Unfortunately this indirect approach of using softening stress-strain relationships has been found to be both size and shape dependent [9-13] which limits its application. Furthermore, the use of these empirically derived softening stress-strain

relationships in the analysis of RC members necessitates the use of empirically derived hinge lengths [14-18] which are themselves difficult to quantify [18].

To overcome the problems mentioned above that are associated with concrete softening, an alternative approach is proposed in this paper for quantifying the softening of concrete. It is shown how the behaviour of compression wedges can be measured directly from compression tests on axially loaded rectangular prisms of varying dimensions in which the deformation or effective strain profile is uniform. Furthermore, it is shown how these results can be used to quantify the behaviour of compression wedges in flexural members where the deformation or effective strain profile is no longer uniform but varies linearly. Hence the effect of the concrete on the ductility, that is the rotation at a hinge, can be quantified from a relatively few number of simple prism tests and used to simulate the formation of hinges in RC members of any cross-section. It is suggested that this may be a useful approach in the development of new concrete products, such as high strength concrete, concrete made from pulverised fly ash or concrete with steel or polymer fibres, if the effect of the concrete on the member ductility is important.

The fundamental principles that govern this wedge based approach are first described for uniformly loaded rectangular sections and it is then shown how it can be applied to flexurally loaded members such as in beams. In order to illustrate this approach, a series of tests for quantifying the wedge behaviour are then described and the results used to analysis the compression region in beams as occurs in eccentrically loaded prisms [4,5]. The aim of this paper is not to specifically quantify the behaviour of concrete softening wedges but to illustrate how the wedge behaviour can be quantified and the results used in flexural members to quantify their rotational capacity.

2. Wedge based model

The wedge based model assumes that the concrete material remains linear elastic, that is it has a constant modulus of E_c , and that any non-linearity that might occur is due to micro-cracking along planes that allows shear deformations associated with shear-friction theory [19-22]. The wedge base model is first explained in the context of a prism as in Fig. 2(a) where the displacements δ_a are applied uniformly along the width of the prism $2d_w$ such

that the effective strain δ_a/L_{def} is uniform across the prism width. The wedge based model is then applied to an eccentrically loaded prism where the displacement δ and effective strain δ/L_{def} vary linearly as occurs in flexural members.

2.1 Rectangular axially loaded prisms

Consider the prism in Fig. 2(a) of height $2L_{def}$ and width $2d_w$. Let us assume that the depth of the prism into the page is very large so that the behaviour of cross-sections within the page are identical which simplifies this to a two-dimensional behaviour. A uniform pressure σ is applied to the horizontal surface which induces a contraction $2\delta_a$ over the depth $2L_{def}$. Each half of the prism behaves identically being subjected to a contraction δ_a over a length L_{def} .

The prism in Fig. 2(a) can be tested to failure and the results plotted as in Fig. 3 where the abscissa will be referred to as the effective strain ε_{eff} which is the measured overall contraction over the prism length that is δ_a/L_{def} in Fig. 2(a). On loading in Fig. 3, the stress/effective-strain relationship may be considered to follow a linear path O-A, with a modulus E_c up to a stress αf_p , after which non-linearity occurs in the ascending portion A-C, where the strength peaks at f_p , followed by a descending portion C-D which is often referred to as softening. In the wedge based model, this non-linearity is associated with the formation of micro-cracks in the region of inclined wedge shaped planes as in Fig. 2(b) which allow shearing across the inclined planes to accommodate the non-linearity shown in Fig. 3. For example, the plane A-F in Fig. 2(b) which contains both B-C and D-E on opposing sides of potential sliding planes, will deform through micro-cracking to allow the deformation shown in Fig. 2(c) where sliding of the wedge from B to C shortens the prism by S_w such that the effective strain due to sliding S_w/L_{def} is the non-linear strain in Fig. 3 which in the ascending branch is shown as $\varepsilon_{n-mic-asc}$ and that in the descending branch as $\varepsilon_{n-mic-des}$. It can be seen in Fig. 2(c) that this sliding action must be accommodated by localised crushing as shown to allow the wedges to move sideways which is the dilation of the member which can be measured [23] but is not the subject of this paper.

In summary, the effective strain ε_{eff} in Fig. 3 consists of the material strain ε_{mat} and that due to micro-cracking ε_{mic} . Another way of visualizing this behaviour is that the

components of the prism A-B, C-D and E-F in Fig. 2(c) when subjected to a stress σ_n can only contract through material contraction δ_{mat} by $\epsilon_{n-mat}L_{def}$ where ϵ_{n-mat} is σ_n/E_c and the remaining deformation δ_S can only be accommodated by wedge sliding S_w such that ϵ_{n-mic} is equal to S_w/L_{def} . Hence the total deformation δ in Fig. 2(c) is the sum of δ_{mat} and δ_S .

The prism in Fig. 2(c) consists of four wedges. Let us consider the single wedge in the upper right quadrant which is shown in Fig. 4. The distance L_{def} is any convenient distance that encapsulates the length of the wedge L_w and d_w is now the depth of the wedge. It can be seen that the uniform displacement δ_n which imposes a stress σ_n causes a uniform slip along the sliding plane that causes a contraction S_n . It can also be seen that the effects of micro-cracking which occurs over a finite region are represented by a sliding action along a plane which is referred to as shear-friction theory. The effective strain ϵ_{n-eff} in the quadrant in Fig. 4 is δ_n/L_{def} which comprises that due to the elastic deformation ϵ_{mat} that is σ_n/E_c and that due to the contraction due to micro-cracking S_n/L_{def} . Hence the contraction due to micro-cracking is given by

$$S = (\epsilon_{eff} - \epsilon_{mat})L_{def} \quad (1)$$

Equation 1 can be used to convert the effective strains which can be measured experimentally, to contractions S due to micro-cracking as in Fig. 5 where S_p is the contraction at the peak stress f_p . Hence the variation in Fig. 5 can be obtained directly from prism tests as in Fig. 2 and used to determine the behaviour of wedges in prisms as in Fig. 4 where the deformation is uniform. However, in beams the deformation is not uniform which is the subject of the following section.

2.2 Flexurally loaded beams

The prism in Fig. 2(a) which is subjected to a concentric load is now subjected to an eccentric load as in Fig. 6. Because of the eccentricity of load, the deformation δ is now no longer uniform but varies from δ_L on the left to δ_R on the right so that there is a linear variation in the effective strains δ/L_{def} and a rotation θ . Because of the eccentricity of load, a

wedge first forms on the loaded side of the prism as shown in which the depth of the wedge d_w is no longer equal to half the width of the prism d .

The bottom half of the prism in Fig. 6 is shown rotated by 90° in the clockwise direction in Fig. 7(e). The surface of the prism, A-A in Fig. 7(d), is now subjected to a compressive deformation at the top δ_T and a tensile deformation at the bottom δ_B such that there is a linear variation of the effective strain ε_{eff} in Fig. 7(c) from δ_T/L_{def} at the top to δ_B/L_{def} at the bottom. Micro-cracking starts at a stress αf_p in Fig. 3; this stress αf_p is shown in Fig. 7(b), the accompanying strain $\alpha f_p/E_c$ in Fig. 7(c), and the accompanying deformation $(\alpha f_p/E_c)L_{def}$ in Fig. 7(d) which is shown as line B-B. Hence any deformation within the prism that is greater than the deformation of line B-B requires micro-cracking. Hence any deformation above point C in Fig. 7(d) requires micro-cracking which, therefore, fixes the depth of the wedge d_w as shown.

Let us first consider the behaviour below point C in Fig. 7(d). The linear deformation C-E produces the effective linear strain distribution F-G-H in Fig. 7(c). If the concrete cracks in tension at ε_{ct} at level G, then the strain distribution F-G is a real strain distribution, that is it is a material strain distribution. Hence, the stresses in this region F-G in Fig. 7(b) can be determined from the concrete modulus. Subsequently, the forces in this region can be determined as in Fig. 7(a) where $F_{el,c}$ is the force in the elastic concrete compression region and $F_{el,t}$ is the force in the elastic tension region. If the concrete cracks in tension at level G in Fig. 7(c), then G-H is an effective strain. If reinforcing bars intercepted this crack, then the force in the reinforcing bar F_r would depend on both the crack width Δ_r in Fig. 7(d) and the bond-slip properties, which is dealt with elsewhere using partial-interaction theory [24-29] as this paper is only dealing with concrete under compression.

Let us now consider the behaviour in the micro-cracking region in Fig. 3 that is above point C in Fig. 7(d). Consider level n where the prism must accommodate the deformation H-I. Part of this deformation H-J is accommodated by concrete material straining ε_{mat} as shown in Fig. 7(c) such that the deformation due to material straining H-J is given by $(\sigma_n/E_c)L_{def}$ and the remaining deformation J-I is due to micro-cracking contraction S_n at the wedge interface as shown in Fig. 7(e). It is simple a question of finding the stress σ_n such that the material contraction $\sigma_n L_{def}/E_c$ plus the micro-cracking contraction

from Fig. 5, S_{n-asc} or S_{n-des} , depending on whether it is in the ascending or descending branch, equals the required deformation H-I in Fig. 7(d). From this analysis of the wedge, where the depth of which d_w is usually divided into segments in which each segmental is assumed to have a uniform stress, the resulting force in the wedge and its position F_w in Fig. 7(a) can be determined.

The resultant of the forces in Fig. 7(a) and its position can now be determined. If the eccentrically loaded prism in Fig. 6 is being analysed, then the resultant of the forces in Fig. 7(a) needs to be in line with P and this can be obtained by pivoting the displacement D-E in Fig. 7(d) about D until the resultant force is in line. If a beam were being analysed, then it is simply a question of pivoting about D until the resultant force was zero.

3. Rectangular prism tests

These tests [23] were performed simply to illustrate how the wedge properties required for the flexural analysis depicted in Fig. 7 could be obtained from prism tests as depicted in Fig. 2; as such they are not meant to be a comprehensive quantification of the wedge properties.

Four different sizes of prisms were chosen [23] with a width ($2d_w$ in Fig. 2(a)) to height ($2L_{def}$) to depth ratio of 1:2:4 as shown in Table 1 and in Fig. 8. Theoretical shear-friction research on the formation of wedges [19] would suggest that the wedge can be contained within prisms of width to height ratio of 1:2 as in Fig. 8(a). If the height were any less with respect to the width then the platen restraints at the ends would affect the angle of wedge that is α in Fig. 7(e). Wedges form as shown in Fig. 8(a) where the wedge forms into the width ($2d_w$) and over the depth of the specimen. However, they also form at the ends and into the depth and over the width ($2d_w$) of the specimen. Deep specimens, that is specimens as in Fig. 8(b) where the depth was much greater than the width, were chosen so that the wedge formation as in Fig. 8(a) would dominate the behaviour so that the behaviour could be assumed to be two-dimensional.

The elastic modulus of the concrete material was derived from standard cylinder tests [23]. The contraction of the specimens were measured with transducers [23] so from Eq. 1 can be derived the contraction due to wedge slip S . Three or four specimens of each

size were tested and the average of the results for each size is plotted in Fig. 9. The average peak stress f_p and contraction at peak stress S_p are recorded in Table 1 and these were used to non-dimensionalise Fig. 9 as shown in Fig. 10. Curve fitting of Fig. 10 gave the following expression for micro-cracking displacement S for a given stress σ

$$\frac{\sigma}{f_p} = \left[-0.65 \left(\frac{S}{S_p} \right)^2 + 5.71 \left(\frac{S}{S_p} \right) + 5.04 \right] EXP \left[0.03 \left(\frac{S}{S_p} \right)^2 - 0.50 \left(\frac{S}{S_p} \right) - 1.87 \right] (2)$$

where f_p had an average value of 43 MPa and S_p was found to be a function of depth of wedge d_w as follows

$$S_p = 0.0025 d_w \quad (3)$$

Equation 2 provided an accurate fit to the experimental results, as shown in Fig. 11.

4. Analysis of eccentrically loaded prism tests

The analysis depicted in Fig. 7 and using the wedge properties in Eqs. 2 and 3 was applied to Daniel et al's test specimens [5]. The specimens as represented in Fig. 6 had a width d of 300mm, height $2L_{def}$ of 360 mm, depth into the page of 180 mm, an average concrete strength of 33 MPa and were tested at eccentricities e of 60, 70 and 85 mm. It may be worth noting that the average concrete strength of the prism used to derive Eqs. 2 and 3 was 43 MPa, hence, the shape of the variations in material properties given by Eqs. 2 and 3 and illustrated in Fig. 11 are really only applicable to this strength of concrete. However, to illustrate this analysis technique it has been applied to Daniel et al's specimens which were a bit weaker at 33 MPa.

A typical comparison of the moment-rotations is shown in Fig. 12. Two experimental tests were performed at this eccentricity and these are shown as unbroken lines; the difference between these tests is a gauge of the scatter that can be expected even from supposedly identical specimens and tests. The test results have been compared with the results of theoretical analyses with variations in concrete strength from 43 MPa to

28MPa and which are shown as broken lines. Bearing in mind the scatter between the test results, it is suggested that the shape of the theoretical results compare well with those of the tests. It can be seen that this new approach can simulate the moment-rotation softening without the need for empirical hinge lengths nor softening stress-strain relationships.

The main interest of this research is the non-linearity due to micro-cracking as already illustrated in Fig. 5 for prism tests. Dividing the abscissa θ of Fig. 12 by L_{def} gives the curvature χ . In which case, the initial stiffness or tangent stiffness of the rising branch in Fig. 12 would be the elastic flexural rigidity EI and divergence from this would be due to flexural cracking and micro-cracking. This divergence due to cracking which is the main interest of this research has been plotted in Figs. 13 to 15 for each test specimen in which the eccentricities were 60, 70 and 85mm. It is suggested that the results show that the model can closely represent softening.

The above wedge based analyses have been applied to eccentrically loaded flexural members without any reinforcement as illustrated in Fig. 6. As already explained in the wedge based analyses depicted in Fig. 7, these analyses could also have been applied to reinforced flexural members where the force in the longitudinal reinforcement is a function of Δ_r in Fig. 7(d) [26, 27 and 29]. It can, therefore, be seen that once the wedge properties, such as those in Eqs. 2 and 3, have been derived from prism tests, as in Fig. 8, they can be used to derive the ductility of any reinforced concrete beam such as that in Fig. 1.

5. Conclusions

Quantifying concrete softening and the region over which softening occurs using softening stress-strain relationships and empirical hinge lengths has proved to be a very difficult problem. An alternative approach is described in which the concrete softening behaviour is measured directly through prism tests; it is shown how the results of these prism tests can be used in the analysis of flexural members without the need for softening stress-strain relationships and without the need for empirical hinge lengths. This approach is unique as it does not require stress-strain softening relationships but stress-sliding relationships that can be obtained directly from prism tests. This new wedge based approach has been compared with tests on eccentrically loaded prisms giving good simulation of the softening behaviour

due to micro-cracking. It is suggested that this direct approach may be useful in the development of new concrete materials such as fibre concrete and maybe also be useful in the refinement of existing ductility models for ordinary reinforced concrete.

Acknowledgements

This research was supported by the Australian Research Council Discovery grant DP0985828 “A unified reinforced concrete model for flexure and shear”. The first author has been financially supported by the Directorate General of Higher Education, Department of National Education of Indonesia through a Master degree.

References

1. Van Vliet MRA, Van Mier JGM (1996) Experimental investigation of concrete fracture under uniaxial compression. *Mechanics of Cohesive-Frictional Materials* 1:115-127
2. Wu C, Oehlers DJ, Rebentrost M, Leach J, Whittaker AS (2009) Blast testing of ultra-high performance fibre concrete slabs and FRP retrofitted RC slabs. *Engineering Structures* 31: 2060-2069
3. Nemecek J, Bittnar Z (2004) Experimental investigation and numerical simulation of post-peak behavior and size effect of reinforced concrete columns. *Materials and Structures* 37: 161-169
4. Debernardi PG, Taliano M (2001) Softening behavior of concrete prisms under eccentric compressive forces. *Magazine of Concrete Research* 53 (4): 239-249
5. Daniell JE, Oehlers DJ, Griffith MC, Mohamed Ali MS, Ozbakkaloglu T (2008) The softening rotation of reinforced concrete members. *Engineering Structures* 30(11): 3159-3166
6. Carreira DJ, Chu KH (1985) Stress-strain relationship for plain concrete in compression. *ACI Journal* 82(6): 797-804
7. Popovics S (1973) Numerical approach to the complete stress-strain relation for concrete. *Cement and Concrete Research* 3(5): 583-599
8. Teng JG, Huang YL, Lam L, Ye LP (2007) Theoretical model for fiber-reinforced polymer confined concrete. *Journal of Composites for Construction* 11(2): 201-210
9. Markeset G, Hillerborg A (1995) Softening of concrete in compression localization and size effects. *Cement and Concrete Research* 25(4): 702-708
10. Jansen DC, Shah SP (1997) Effect of length on compressive strain softening of concrete. *Journal of Engineering Mechanics* 123 (1): 25-35
11. Van Mier JGM (1986) Multiaxial strain-softening of concrete. *Matériaux et Constructions* 19: 179-190
12. Weiss WJ, Guler K, Shah SP (2001) Localization and size-dependent response on reinforced concrete beams. *ACI Structural Journal* 98 (5): 686-695

-
13. Borges JUA, Subramaniam KV, Weiss WJ, Shah SP, Bittencourt TN (2004) Length effect on ductility of concrete in uniaxial and flexural compression. *ACI Structural Journal* 101 (6): 765-772
 14. Baker ALL (1956) *Ultimate load theory applied to the design of reinforced and prestressed concrete frames*. Concrete Publication Ltd London, pp. 91
 15. Sawyer HA (1964) Design of concrete frames for two failure states. *Proceedings of the international symposium on the flexural mechanics of reinforced concrete ASCE-ACI*: 405-31
 16. Corley GW (1966) Rotational capacity of reinforced concrete beams. *Journal Structural Engineering ASCE* 92(ST 10): 121-46
 17. Priestly MJN, Park P (1987) Strength and ductility of concrete bridge columns under seismic loading. *ACI Structural Journal* (Jan-Feb) Title no. 86-58: 61-76
 18. Panagiotakos TB, Fardis MN (2001) Deformation of reinforced concrete members at yielding and ultimate. *ACI Structural Journal* 98(2): 135-48
 19. Mohamed Ali MS, Oehlers DJ, Griffith MC (2010) The residual strength of confined concrete. *Advances in Structural Engineering* 13(4): 603-618
 20. Haskett M, Oehlers DJ, Mohamed Ali MS, Sharma SK (2011) The shear-friction aggregate-interlock resistance across sliding planes in concrete. *Magazine of Concrete Research* 62(12): 907-924
 21. Haskett M, Oehlers DJ, Mohamed Ali MS, Sharma SK (2011) Evaluation the shear-friction resistance across sliding planes in concrete. *Engineering Structures* 33: 1357-1364
 22. Lucas W, Oehlers DJ, Mohamed Ali MS, Griffith MC (2011) The FRP reinforced concrete shear-friction mechanism. *Accepted Advances in Structural Engineering*
 23. Nurwidayati R (2011) *An Empirical Approach to Simulate the Concrete Softening Mechanism in RC members*. Master thesis, The University of Adelaide (to be submitted in August 2011)
 24. Haskett M, Oehlers Dj, Mohamed Ali MS, Wu C (2009a) Rigid body moment-rotation mechanism for reinforced concrete beam hinges. *Engineering Structures* 31(5): 1032-1041

-
25. Haskett M, Oehlers DJ, Mohamed Ali, Wu C (2009) Yield penetration hinge rotation in reinforced concrete beams. *ASCE Structural Journal* 135(2): 130-138
 26. Haskett M, Mohamed Ali MS, Oehlers DJ, Wu C (2009) Influence of bond on the hinge rotation of FRP plated beams. *Special edition of Advances in Structural Engineering* 12(6): 833-843
 27. Muhamad R, Mohamed Ali MS, Oehlers DJ, Sheikh AH (2011) Load-slip relationship of tension reinforcement in reinforced concrete members. *Engineering Structures* 33: 1098-1106
 28. Visintin P, Oehlers DJ, Wu C, Haskett M. A mechanics solution for hinges in RC beams with multiple cracks. *Submitted Engineering Structures* 17/6/11
 29. Muhamad R, Mohamed Ali MS, Oehlers DJ, Griffith MC. The tension stiffening mechanism in reinforced concrete prisms. *Submitted International Journal of Advances in Structural Engineering*

Table 1 Detail of concrete prisms

Prism	Width [2d_w] (mm)	Height [2L_{def}] (mm)	Depth (mm)	S_p (mm)	f_p (mm)
Test-50	50	100	200	0.04	45
Test-75	75	150	300	0.11	48
Test-100	100	200	400	0.12	42
Test-125	125	250	500	0.15	39



Fig. 1 Compression wedge in a beam [2]

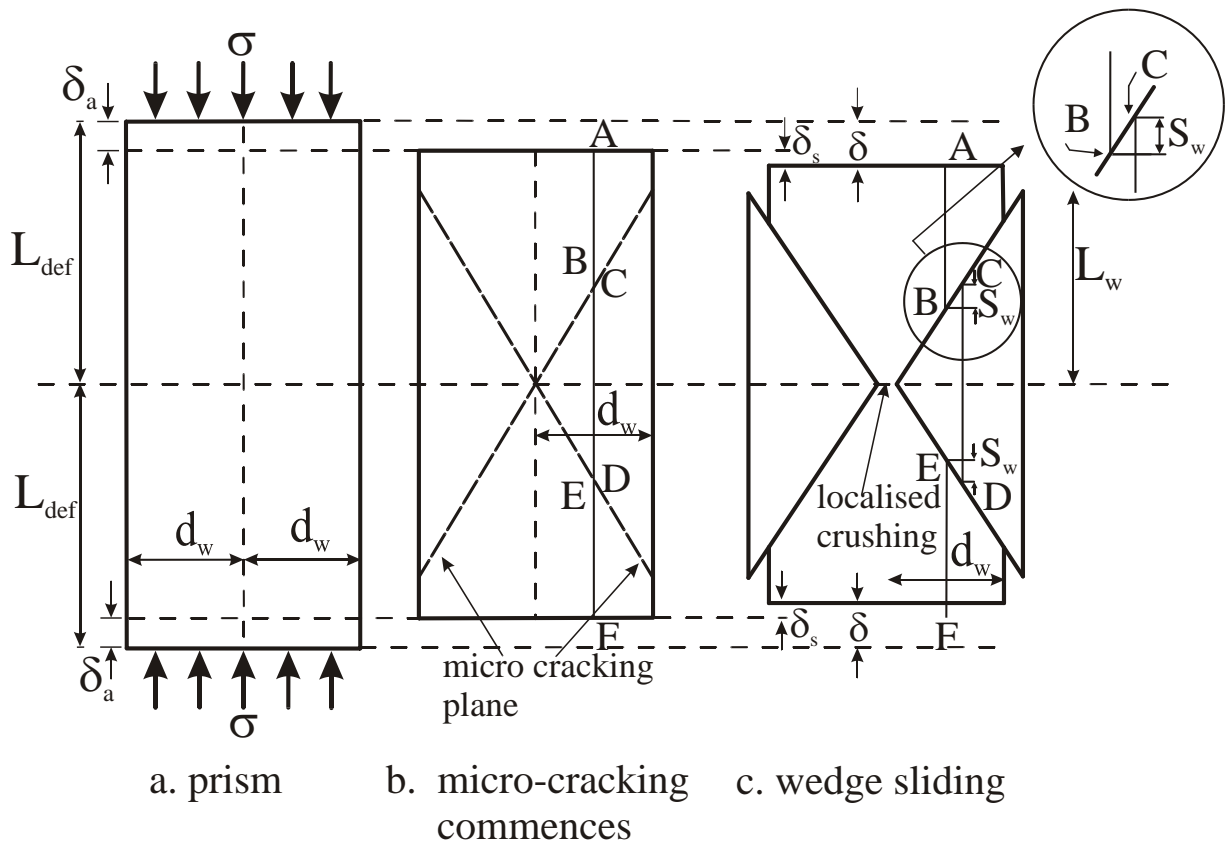


Fig. 2 Concentrically loaded prism

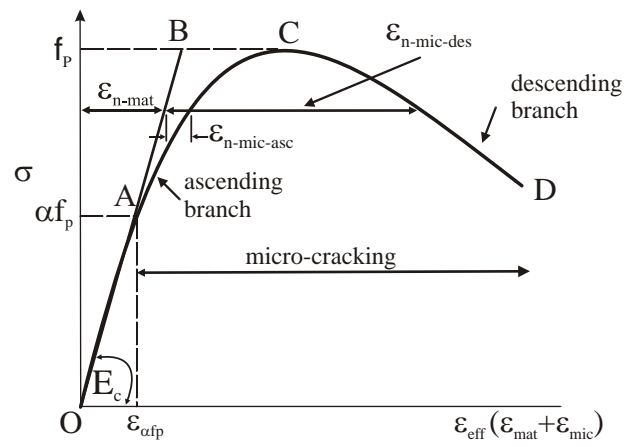


Fig. 3 Measured concrete material properties

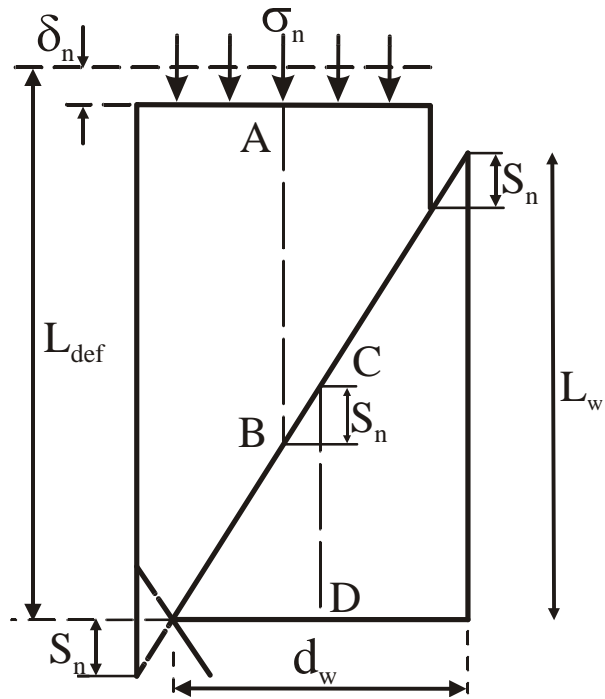


Fig. 4 Deformation of a single wedge

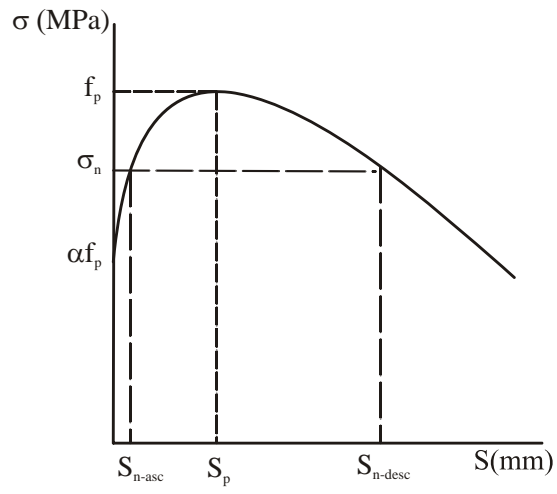


Fig. 5 Wedge contractions

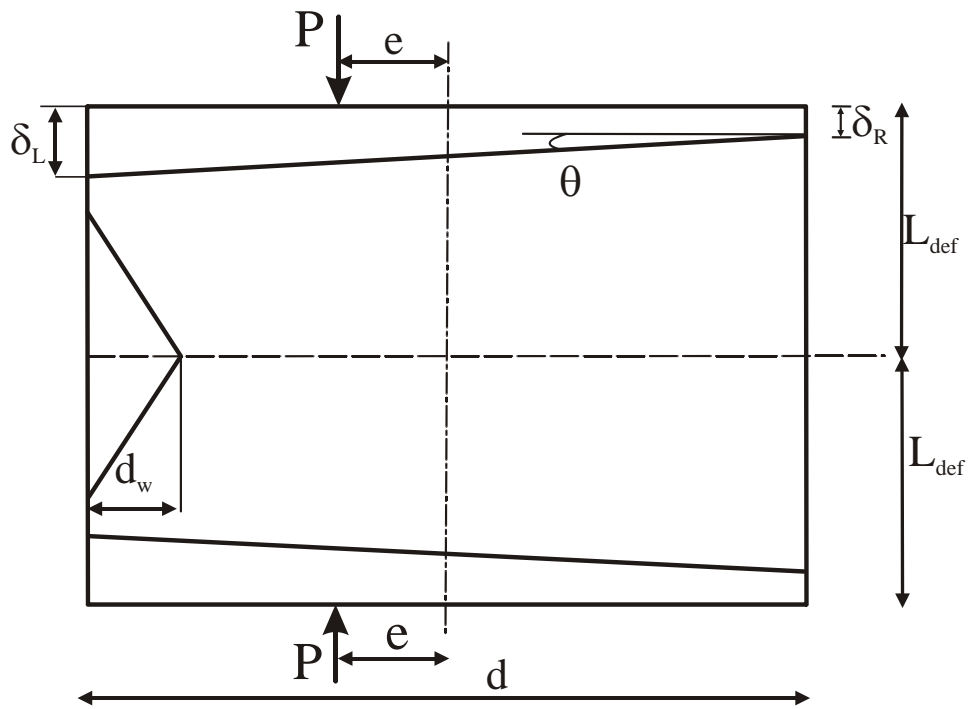
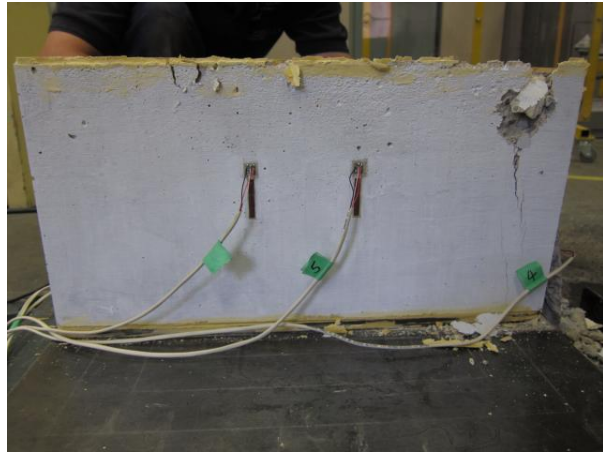


Fig. 6 Eccentrically loaded prism



(a). Width ($2d_w$) to height ($2L_{def}$)



(b). depth to height

Fig. 8 Typical formation of wedges

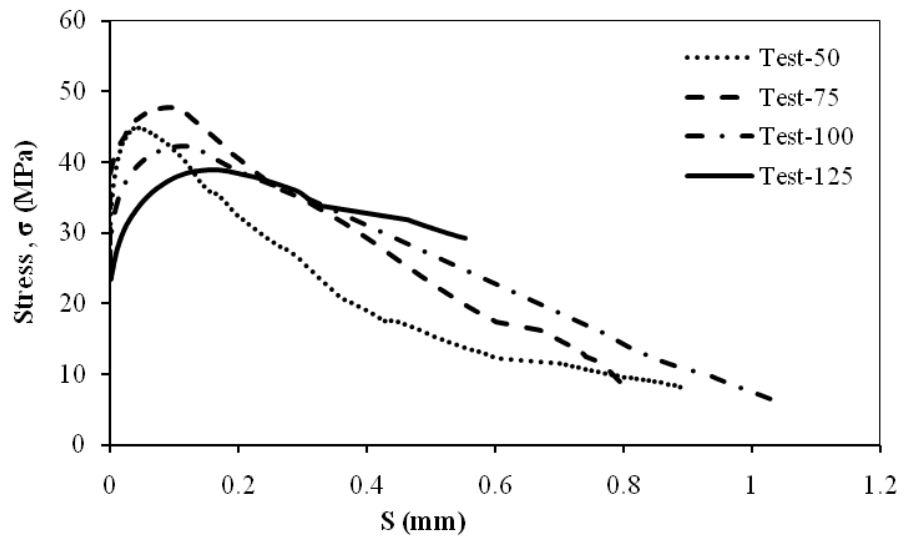


Fig. 9 Test results

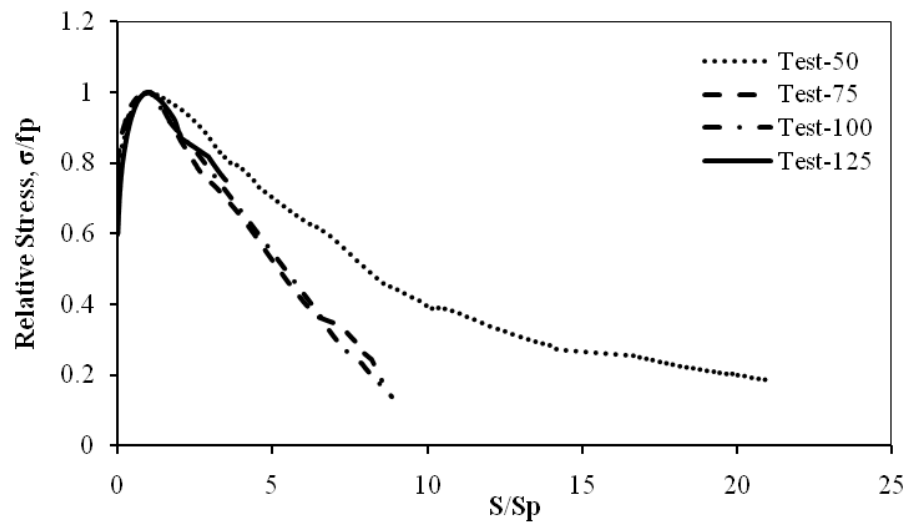


Fig. 10 Non-dimensionalised test results

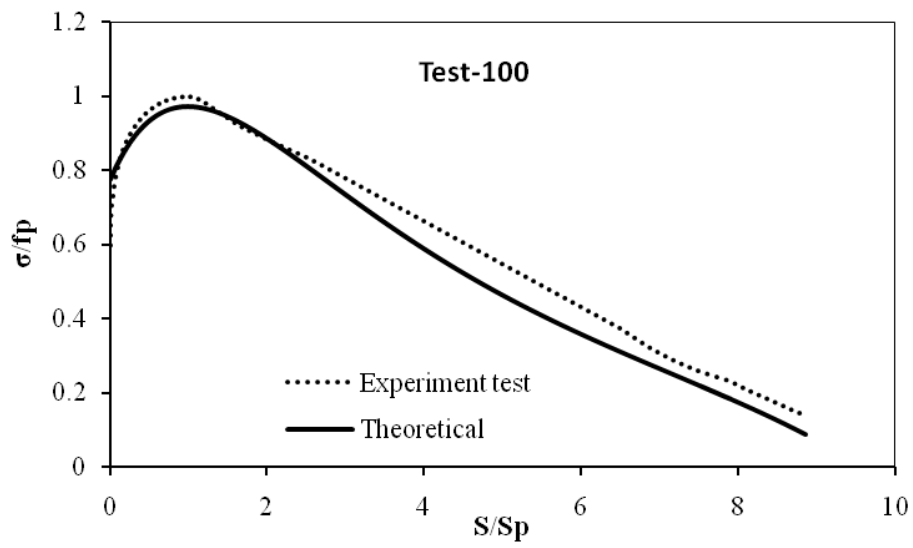


Fig. 11 Stress-slip comparison

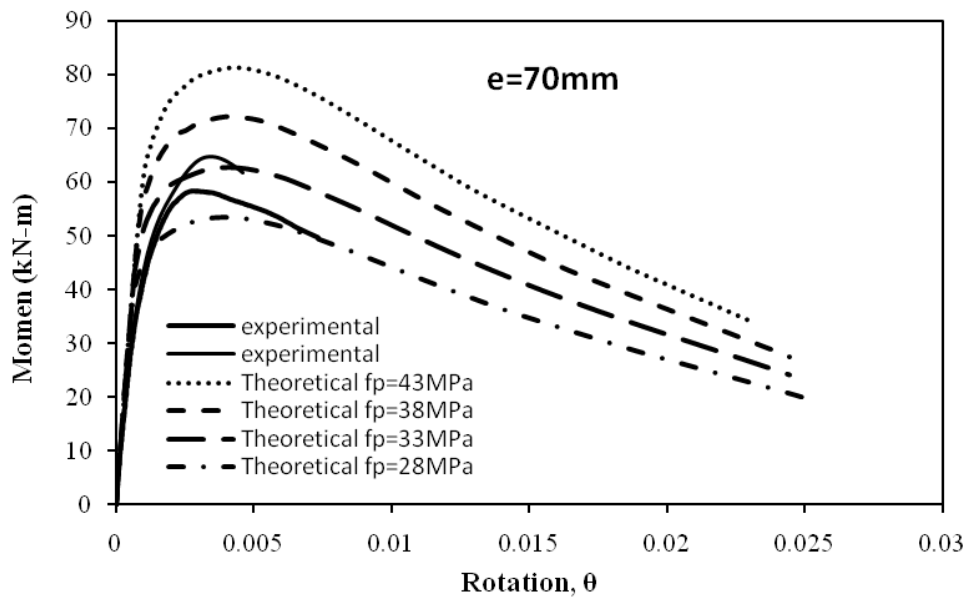


Fig. 12 Typical moment-rotation comparison

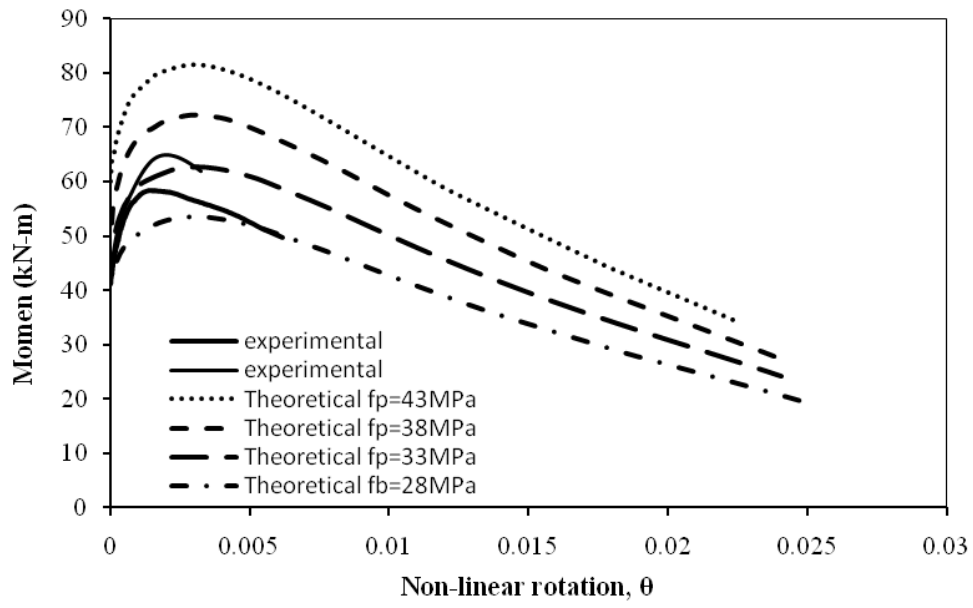


Fig. 13 Non-linear rotation at $e = 70\text{ mm}$

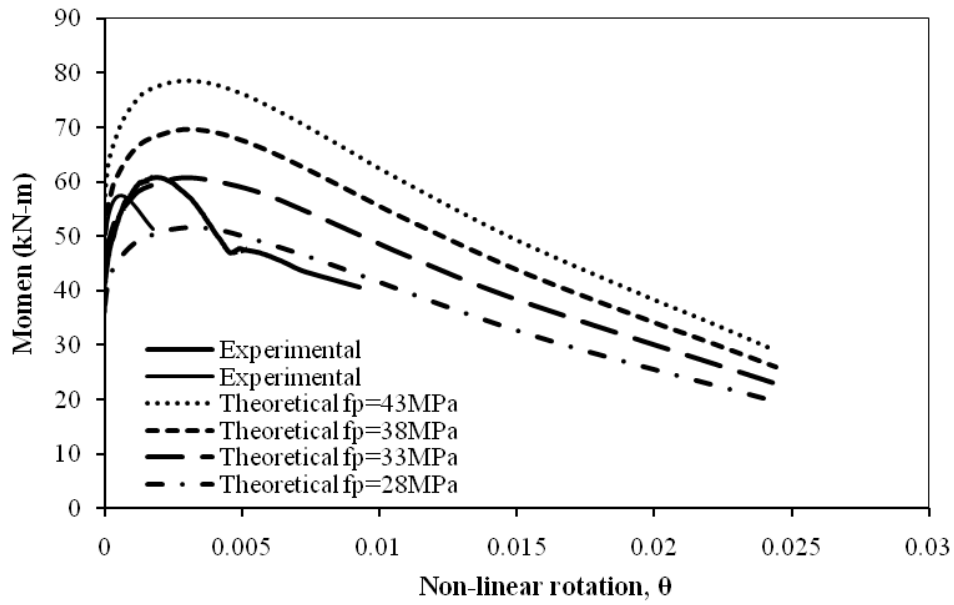


Fig. 14 Non-linear rotation at $e = 60$ mm

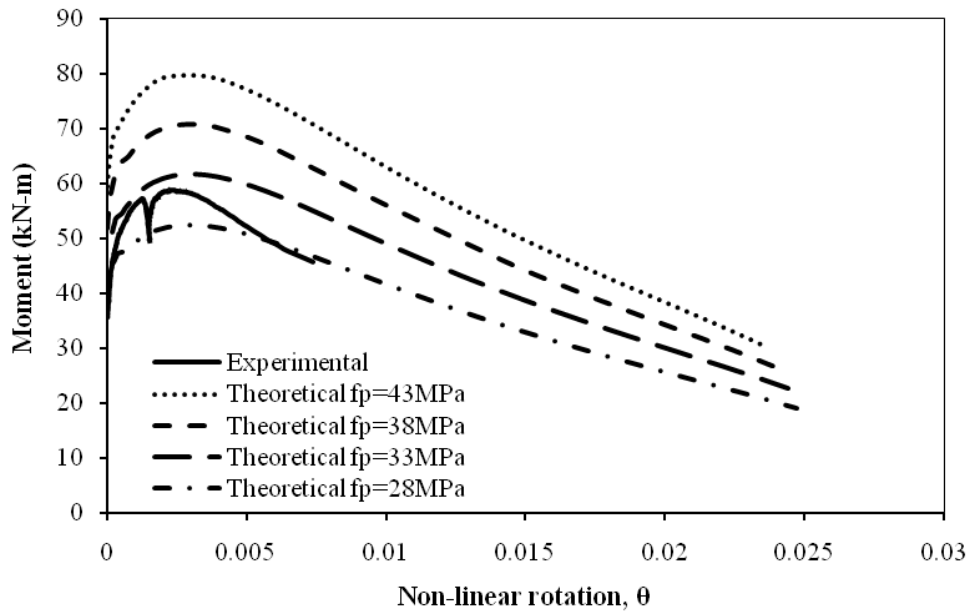


Fig. 15 Non-linear rotation at $e = 85$ mm



ACKNOWLEDGEMENT

The work written in this thesis was carried out at the University of Adelaide in the Department of Civil, Environmental and Mining Engineering under the supervision of Dr. Chengqing Wu, Professor Deric Oehlers, Dr. Matthew Haskett.

It is a pleasure to thank those who made this thesis possible Dr. Chengqing Wu, Professor Deric Oehlers, Dr. Matthew Haskett for their encouraging, continuing supervision, extraordinary guidance and patience throughout this research from the initial to the final level. Their contribution and supervision enabled me to develop an understanding and complete this research. I also would like to thank them for their commitment to organize weekly meeting to give me invaluable discussion and ideas.

I am grateful for assistance and support from all of the laboratory staff in the Civil, Environmental and Mining Engineering Department, especially to David Hale, Ian Cates, Steven Huskinson and Jon Ayoub for their professional advises and patience throughout the experimental program. I am also thankful to Stephen Carr for providing computing assistance, Barbara Brougham for editing some chapters of this thesis.

I would like to thank to Indonesian Government through Directorate General of Higher Education, Department of National Education of Indonesia for their financially supported.

Special thanks are extended to my graduate friends, especially Rahimah Muhamad, Phillip Visintin, Bambang Setiawan, Nora Abdullah and Yunita Idris for their assistance, friendship, encouragement and support during the entire period of research.

Deepest thanks and appreciation to my family, my beloved husband Khairil Fiannor Ansyari and son Yuqo Azhari Alifanur for their endless love, encouragement, understanding and continuous support through the duration of my study.

Last but not least I dedicates this thesis to my beloved parents Abdul Djebar Hapip dan Kesuma Sekarsih.



Table of Contents

ABSTRACT	i
STATEMENT ORIGINALITY	ii
LIST OF PUBLICATION	iii
PUBLICATION	iv
ACKNOWLEDGEMENT	xxxv
TABLE OF FIGURES	xxxix
TABLE OF TABLES.....	lvii
Chapter 1: INTRODUCTION	1
Chapter 2: LITERATURE REVIEW	3
2.1 Stress-Strain Properties of Concrete in Compression	3
2.1.1 Material Deformation.....	4
2.1.2 Strain Softening.....	5
2.2 Shear Friction Theory.....	15
Chapter 3: PRISM SOFTENING EXPERIMENTS- $f_c=38\text{MPa}$	19
3.1 Introduction.....	19
3.2 Design of Specimens	19
3.2.1 Material Properties	19
3.2.2 Specimens Detail.....	31
3.2.3 The Test Rig and Instrumentation	32
3.3 Test Results.....	35
3.4 Analysis of Test Results	57
3.4.1 Method of analysis	57
3.4.2 Individual tests.....	70
3.4.3 Comparison of Axial Deformation.....	143
3.4.4 Comparison of Lateral Deformation	160
3.4.5 Wedges Analysis	176
Chapter 4: PRISM SOFTENING EXPERIMENTS- $f_c=23\text{MPa}$	187
4.1 Introduction.....	187
4.2 Design of Spesimens	187
4.2.1 Material Properties	187

4.2.2 Specimens Detail	191
4.2.3 The Test Rig and Instrumentation	192
4.3 Test Results	194
4.4 Analysis of Test Results	224
4.4.1 Method of analysis	224
4.4.2 Individual tests.....	224
4.4.3 Comparison of Axial Deformation	267
4.4.4 Comparison of Lateral Deformation.....	275
4.4.5 Wedges Analysis	283
Chapter 5: MOMENT ROTATION ANALYSIS.....	299
5.1 Introduction.....	299
5.2 Concentrically Loaded Prisms	299
5.3 Eccentrically Loaded Beams.....	301
5.3.1 Elastic Condition	302
5.3.2 Non-elastic Condition	307
5.3.3 The Results and Validation.....	312
Chapter 6: CONCLUSION	319
REFERENCES	323
NOTATION.....	329

TABLE OF FIGURES

Figure 2.1:	A typical compression stress-strain relationship of concrete	3
Figure 2.2:	Effect of parameter n to stress strain relationship.....	6
Figure 2.3:	Localisation behaviour of concrete in compression	7
Figure 2.4:	Relationship between relative/normalised stress and post peak deformation (Jansen and Shah, 1995 and Van Vliet and Van Mier 1996).....	9
Figure 2.5:	The compressive strength for different slenderness ratio (Van Mier et al. 1997)	11
Figure 2.6:	Confined zones due to frictional restraint for specimens of different slenderness (Van Vliet and Van Mier 1996)	12
Figure 2.7:	Effect of slenderness ratio and frictional restraint (König et al 1994).....	12
Figure 2.8:	Comparison of stress-strain relationship of prisms of different size and slenderness ratio and loaded between rigid steel platens (Gobbi and Ferrara (1995)	15
Figure 2.9:	Concrete softening wedge	17
Figure 3.1:	(a) Seidner Compression Testing Machine; (b) concrete cylinder	20
Figure 3.2:	The diagram of transducers and strain gauges layout: (a) side view; (b) top view	21
Figure 3.3:	(a) how to produce the mortar; (b) fresh mortar; (c) separate aggregate; (d) 100mm×200mm mortar cylinder	22
Figure 3.4:	(a) rock sample; (b) 58mm diameter and 150mm length core aggregate cylinder; (c) aggregate test set up	23
Figure 3.5:	Stress-axial strain relationship of six concrete cylinders.	24
Figure 3.6:	The average of the six stress-axial strain relationship curves of concrete cylinders.	25
Figure 3.7:	Failure pattern of concrete cylinder	25
Figure 3.8:	Stress-axial strain response of five mortar cylinders.....	26
Figure 3.9:	The average of stress – axial strain relationship of mortar cylinders.	27
Figure 3.10:	Failure pattern for mortar cylinders	27
Figure 3.11:	Stress–slip wedge response of five core aggregate cylinders.	28
Figure 3.12:	The average curve of stress-slip wedge response of core aggregate cylinders. ...	29

Figure 3.13: Failure pattern of core aggregate cylinders.....	29
Figure 3.14: Comparison the stress-strain of concrete, mortar and aggregate.	30
Figure 3.15: The geometry of the concrete prism.....	31
Figure 3.16: Amsler Compression Test Machine.....	33
Figure 3.17: Diagram of axial and lateral transducer layout on prism.	33
Figure 3.18: Prism uniaxial compression test setup.	34
Figure 3.19: Total axial load (L) applied to the prism.....	36
Figure 3.20: The dilation of the prism (top view of prism).....	37
Figure 3.21: Relationship between total axial load and contraction graph of Test1-125.....	38
Figure 3.22: Total axial load – dilation response of Test1-125.....	38
Figure 3.23: Failure pattern of concrete prism Test1-125; (a) failure on one face; (b) side view	39
Figure 3.24: The response of total axial load and contraction for Test2-125.....	40
Figure 3.25: Total axial load – dilation response of prism Test2-125.	40
Figure 3.26: Failure pattern of concrete Test2-125: (a) front view; (b) side view; (c) top view	41
Figure 3.27: Total axial load-contraction response of prism Test3-125.....	41
Figure 3.28: Total axial load – dilation response of prism Test3-125.	42
Figure 3.29: Failure pattern of concrete prism Test3-125; (a) front view; (b) side view.....	42
Figure 3.30: Total axial load (L) contraction response of prism Test4-125.	43
Figure 3.31: Total axial load– dilation response of prism Test4-125.	43
Figure 3.32: Failure pattern of concrete prism Test4-125; (a) front view; (b) side view; (d) top view.	44
Figure 3.33: Total axial load - contraction response of Test5-100	44
Figure 3.34: Total axial load – dilation response of prism Test5-100	45
Figure 3.35: Failure pattern of concrete Test5-100	45
Figure 3.36: Relationship between total axial load and contraction for prism Test6-100.	46
Figure 3.37: Total axial load – dilation response of prism Test6-100.	47
Figure 3.38: Failure pattern of concrete Test6-100; (a) front view; (b) side view.	47
Figure 3.39: The relationship between total axial load and contraction of prism Test7-100 ...	48
Figure 3.40: Total axial load–dilation response of Test7-100.....	48

Figure 3.41: Failure pattern of concrete prism Test7-100; (a) front view; (b) and (c) sides view	49
Figure 3.42: Total axial load-contraction response of Test8-75	49
Figure 3.43: Total axial load–dilation response of Test8-75.	50
Figure 3.44: Failure pattern of concrete prism Test8-75; (a) front view; (b) side view.....	50
Figure 3.45: Total axial load-contraction response of prism Test9-75.....	51
Figure 3.46: Total axial load-dilation response of prism Test9-75.....	51
Figure 3.47: Failure pattern of concrete prism Test9-75; (a) and (b) front view; (c) side view	52
Figure 3.48: The relationship of total axial load-contraction of prism Test10-75	52
Figure 3.49: Total axial load–dilation response of Test10-75.	53
Figure 3.50: Failure pattern of concrete Test10-75; (a) front view; (b) sides view.	53
Figure 3.51: Total axial load and contraction response of Test11-50.....	54
Figure 3.52: Total axial load (L) – dilation response of Test11-50.	54
Figure 3.53: Failure pattern of concrete test11-50; (a) and (b) both faces failed; (c) side view.	55
Figure 3.54: Total axial load and contraction response of Test13-50.....	55
Figure 3.55: Total axial load–dilation response of Test13-50.	56
Figure 3.56: Failure pattern of concrete Test13-50	56
Figure 3.57: The concrete prism under compression load	58
Figure 3.58: A typical of total axial load and total axial contraction of concrete prism.....	58
Figure 3.59: The correction of total axial contraction due to settling down.....	59
Figure 3.60: A typical of L-C response after correction the x-axis	59
Figure 3.61: Idealised wedges of the prism	60
Figure 3.62: Idealised one wedge of prism.....	61
Figure 3.63: The axial load and total axial contraction over one single wedge response.....	62
Figure 3.64: A typical of the relationship axial load P and the slip wedge S_w	64
Figure 3.65: Idealised the wedge per 1 millimeter thickness.....	65
Figure 3.66: A typical response of the wedge load P_w and slip wedge S_w	65
Figure 3.67: The typical of wedge stress – slip wedge response	66
Figure 3.68: A typical total axial load (L) and total lateral expansion (E) response.....	67

Figure 3.69: A typical response of the axial load and total lateral expansion of one single wedge.....	68
Figure 3.70: A typical of the relationship axial load and the wedge expansion V_w	69
Figure 3.71: A typical response of the wedge load and wedge expansion.....	69
Figure 3.72: A typical response of the stress wedge and wedge expansion.....	70
Figure 3.73: The relationship between total axial load and total axial contraction of prism Test1-125.	71
Figure 3.74: The total axial load-total axial contraction response of prism Test1-125 (new axis).	72
Figure 3.75: The axial load -total axial contraction over a single wedge response of prism Test1-125.	73
Figure 3.76: Axial load over one wedge-slip wedge response of prism Test1-125.....	73
Figure 3.77: Load wedge–slip wedge response of prism Test1-125.	74
Figure 3.78: The stress wedge-slip wedge response of prism Test1-125.....	74
Figure 3.79: Total axial load-total lateral expansion response of prism Test1-125.	75
Figure 3.80: The axial load -total lateral expansion over a single wedge response of prism Test1-125	75
Figure 3.81: Axial load-wedge expansion of prism Test1-125.....	76
Figure 3.82: The wedge load-expansion per mm thickness of the wedge for Test1-125	77
Figure 3.83: Wedge stress - wedge expansion of prism Test1-125. x	77
Figure 3.84: Total axial load-total axial contraction response of prism Test2-125.....	78
Figure 3.85: Total axial load-total axial contraction of prism of Test2-125 (new axis).	78
Figure 3.86: The axial load and total axial contraction over one wedge response of prism Test2-125.....	79
Figure 3.87: Axial load-slip wedge response of prism Test2-125.	79
Figure 3.88: Load and slip of wedge response of prism Test2-125.....	80
Figure 3.89: Stress wedge-slip wedge response of prism Test2-125.....	80
Figure 3.90: Total axial load-total lateral expansion response of prism Test2-125	81
Figure 3.91: Axial load-total lateral expansion over one wedge response of prism Test2-125....	81
Figure 3.92: Axial load-wedge expansion response of prism Test2-125.	82

Figure 3.93: Load wedge–wedge expansion response of prism Test2-125.	82
Figure 3.94: Stress wedge – wedge expansion response of Test2-125	83
Figure 3.95: Total axial load-total axial contraction response of prism Test3-125.	84
Figure 3.96: Total axial load-total axial contraction response of prism Test3-125	84
Figure 3.97: Axial load – C/2 slip response of prism Test3-125.	85
Figure 3.98: Axial load-slip wedge response of Test3-125	85
Figure 3.99: Load wedge-slip wedge response of prism Test3-125.	86
Figure 3.100: Stress wedge-slip wedge response of prism Test3-125	86
Figure 3.101: Total axial load-total lateral expansion response of prism Test3-125.	87
Figure 3.102: Axial load – E/2 response of prism Test3-125	87
Figure 3.103: Axial load-wedge expansion response of prism Test3-125.	88
Figure 3.104: Load wedge-wedge expansion response of prism Test3-125.	88
Figure 3.105: Axial stress - wedge expansion response of prism Test3-125.	89
Figure 3.106: Total axial load-total axial contraction response of prism Test4-125	90
Figure 3.107: Total axial load-total axial contraction response of Test4-125 (new axis)	90
Figure 3.108: Axial load – C/2 response of prism Test4-125.	90
Figure 3.109: Axial load-slip wedge response of Test4-125	91
Figure 3.110: Load wedge-slip wedge response of Test4-125	91
Figure 3.111: Axial stress - slip wedge response of prism Test4-125.	92
Figure 3.112: Total axial load-total lateral expansion response of prism Test4-125.	92
Figure 3.113: Load – E/2 response of prism Test4-125.	93
Figure 3.114: Load-wedge expansion response of prism Test4-125.	93
Figure 3.115: Load wedge-wedge expansion response of prism Test4-125.	94
Figure 3.116: Axial stress - wedge expansion response of prism Test4-125.	94
Figure 3.117: Total axial load-total axial contraction response of prism Test5-100	96
Figure 3.118: Total axial load-total axial contraction response of prism Test5-100 (new axis)	97
Figure 3.119: Axial load – C/2 response of prism Test5-100.	97
Figure 3.120: Axial load-slip wedge response of prism Test5-100.	98
Figure 3.121: Load wedge-slip wedge response of prism Test5-100.	98
Figure 3.122: Wedge stress - wedge expansion response of prism Test5-100	99
Figure 3.123: Total axial load-total lateral expansion response of prism Test5-100.	99

Figure 3.124: Axial load – E/2 response of prism Test5-100	100
Figure 3.125: Axial load-wedge expansion response of prism Test 5-100	100
Figure 3.126: Load wedge – wedge expansion response of prism Test5-100	101
Figure 3.127: Stress wedge – wedge expansion response of prism Test5-100.....	101
Figure 3.128: Total axial load-total axial contraction response of prism Test6-100	102
Figure 3.129: Total axial load-total axial contraction response of prism Test6-100 (new axis)	102
Figure 3.130: Axial load – C/2 response of prism Test6-100.....	103
Figure 3.131: Axial load-slip wedge response of prism Test6-100.....	103
Figure 3.132: Load wedge-slip wedge response of prism Test6-100.....	104
Figure 3.133: Stress wedge – slip wedge response of prism Test6-100.....	104
Figure 3.134: Total axial load-total lateral expansion response of Test6-100	105
Figure 3.135: Axial load – E/2 response of prism Test6-100	105
Figure 3.136: Axial load-wedge expansion response of prism Test6-100.....	106
Figure 3.137: Load wedge-wedge expansion response of prism Test6-100.....	106
Figure 3.138: stress wedge-wedge expansion response of prism Test6-100	107
Figure 3.139: Total axial load-total axial contraction response of prism Test7-100	107
Figure 3.140: Total axial load-total axial contraction response of prism Test7-100 (new axis)	108
Figure 3.141: Axial load – C/2 response of prism Test7-100.....	108
Figure 3.142: Axial load-slip wedge response of prism Test7-100.....	109
Figure 3.143: Load wedge-slip wedge response of prism Test7-100.....	109
Figure 3.144: Axial stress - slip wedge response of prism Test7-100.....	110
Figure 3.145: Total axial load-total lateral expansion response of prism Test7-100.....	110
Figure 3.146: Axial load – E/2 response of prism Test7-100	111
Figure 3.147: Axial load-wedge expansion response of Test7-100	111
Figure 3.148: Wedge load-wedge expansion response of Test7-100.....	112
Figure 3.149: Stress wedge – wedge expansion response of prism Test7-100.....	112
Figure 3.150: Total axial load-total axial contraction response of Test8-75.....	114
Figure 3.151: Total axial load-total axial contraction response of Test8-75 (new axis)	115
Figure 3.152: Axial load – C/2 response of prism Test8-75	115

Figure 3.153: Axial load-slip wedge response of prism Test8-75.....	116
Figure 3.154: Load wedge-slip wedge response of prism Test8-75.....	116
Figure 3.155: Axial stress - slip wedge response of prism Test8-75.....	117
Figure 3.156: Total axial load-total lateral expansion response of prism Test8-75.....	117
Figure 3.157: Axial load - E/2 response of prism Test8-75.....	118
Figure 3.158: Axial load-wedge expansion response of prism Test8-75.....	118
Figure 3.159: load wedge-wedge expansion response of prism Test8-75	119
Figure 3.160: Axial stress –wedge expansion response of prism Test8-75	119
Figure 3.161: Total axial load-total axial contraction response of prism Test9-75	120
Figure 3.162: Total axial load-total axial contraction response of Test9-75 (new axis)	120
Figure 3.163: Axial load – C/2 response of Test9-75	121
Figure 3.164: Axial load-slip wedge response of Test9-75	121
Figure 3.165: Load wedge-slip wedge response of prism Test9-75.....	122
Figure 3.166: Stress wedge – slip wedge response of prism Test9-75.....	122
Figure 3.167: Total axial load-total lateral expansion response of Test9-75	123
Figure 3.168: Axial load – E/2 response of Test9-75	123
Figure 3.169: Axial load-wedge expansion response of Test9-75	124
Figure 3.170: Load wedge-wedge expansion response of Test9-75	124
Figure 3.171: Stress wedge – wedge expansion response of Test9-75	125
Figure 3.172: Total axial load-total axial contraction response of Test10-75.....	125
Figure 3.173: Total axial load-total axial contraction response of Test10-75 (new axis)	126
Figure 3.174: Axial load – C/2 response of Test10-75	126
Figure 3.175: Axial load-slip wedge response of Test10-75	127
Figure 3.176: Load wedge-slip wedge response of Test10-75	127
Figure 3.177: Stress wedge – slip wedge response of Test10-75.....	128
Figure 3.178: Total axial load-total lateral expansion response of Test10-75	128
Figure 3.179: Axial load – E/2 response of Test10-75	129
Figure 3.180: Axial load-wedge expansion response of Test10-75	129
Figure 3.181: Load wedge-wedge expansion response of Test10-75	130
Figure 3.182: Stress wedge – wedge expansion response of Test10-75	130
Figure 3.183: Total axial load-total axial contraction response of Test11-50.....	132

Figure 3.184: Total axial load-total axial contraction response of Test11-50 (new axis)	132
Figure 3.185: Axial load – C/2 response of Test11-50	133
Figure 3.186: Axial load-slip wedge response of Test11-50.	133
Figure 3.187: Load wedge-slip wedge response of Test11-50	134
Figure 3.188: Stress wedge – slip wedge response of Test11-50	134
Figure 3.189: Total axial load-total lateral expansion response of Test11-50	135
Figure 3.190: Axial load - E/2 response of Test11-50	135
Figure 3.191: Axial load-wedge expansion response of Test11-50	136
Figure 3.192: Load wedge-wedge expansion response of Test11-50	136
Figure 3.193: Stress wedge-wedge expansion response of Test11-50.....	137
Figure 3.194: Total axial load-total axial contraction response of Test13-50.....	137
Figure 3.195: Total axial load-total axial contraction response of Test13-50 (new axis)	138
Figure 3.196: Axial load – C/2 response of Test13-50	138
Figure 3.197: Axial load-slip wedge response of Test13-50	139
Figure 3.198: Load wedge-slip wedge response of Test13-50	139
Figure 3.199: Axial stress - slip wedge response of Test13-50	140
Figure 3.200: Total axial load-total lateral expansion response of Test13-50	140
Figure 3.201: Axial load - E/2 response of Test13-50	141
Figure 3.202: Axial load-wedge expansion response of Test13-50	141
Figure 3.203: Load wedge-wedge expansion response of Test13-50	142
Figure 3.204: Stress wedge-wedge expansion response of Test13-50.....	142
Figure 3.205: Total axial load-total axial contraction responses of prisms Test-125	144
Figure 3.206: Total axial load-total axial contraction response of Test-100.....	145
Figure 3.207: Total axial load-total axial contraction response of Test-75	145
Figure 3.208: Total axial load-total axial contraction response of Test-50.....	146
Figure 3.209: The average of total axial load-total axial contraction graph.....	147
Figure 3.210: Axial load-C/2 response of Test-125	148
Figure 3.211: Axial load-C/2 response of Test-100	148
Figure 3.212: Axial load-C/2 response of Test-75	149
Figure 3.213: Axial load-C/2 response of Test-50	149
Figure 3.214: The average of axial load-C/2 graph.....	150

Figure 3.215: Axial load-slip wedge response of Test-125	151
Figure 3.216: Axial load-slip wedge response of Test-100	151
Figure 3.217: Axial load-slip wedge response of Test-75	152
Figure 3.218: Axial load-slip wedge response of Test-50	153
Figure 3.219: The average of axial load-slip wedge graph.....	153
Figure 3.220: Load wedge-slip wedge response of Test-125	154
Figure 3.221: Load wedge-slip wedge response of Test-100	155
Figure 3.222: Load wedge-slip wedge response of Test-75	155
Figure 3.223: Load wedge-slip wedge response of Test-50	156
Figure 3.224: The average of load wedge-slip wedge graph.....	156
Figure 3.225: Stress wedge-slip wedge response of Test-125.....	157
Figure 3.226: Stress wedge-slip wedge response of Test-100.....	158
Figure 3.227: Stress wedge-slip wedge response of Test-75.....	158
Figure 3.228: Stress wedge-slip wedge response of Test-50.....	159
Figure 3.229: The average of stress wedge-slip wedge graph.....	160
Figure 3.230: Total axial load-total lateral expansion response of Test-125	161
Figure 3.231: Total axial load-total lateral expansion response of Test-100	161
Figure 3.232: Total axial load-total lateral expansion response of Test-75	162
Figure 3.233: Total axial load-total lateral expansion response of Test-50	162
Figure 3.234: The average of total axial load-total lateral expansion graph.....	163
Figure 3.235: Axial load-E/2 response of Test-125	164
Figure 3.236: Axial load-E/2 response of Test-100	164
Figure 3.237: Axial load-E/2 response of Test-75	165
Figure 3.238: Axial load-E/2 response of Test-50	165
Figure 3.239: The average of axial load-E/2 graph.....	166
Figure 3.240: Axial load-wedge expansion response of Test-125	167
Figure 3.241: Axial load-wedge expansion response of Test-100	167
Figure 3.242: Axial load-wedge expansion response of Test-75	168
Figure 3.243: Axial load-wedge expansion response of Test-50	168
Figure 3.244: The average of axial load-wedge expansion graph.....	169
Figure 3.245: Load wedge-wedge expansion response of Test-125	169

Figure 3.246: Load wedge-wedge expansion response of Test-100	170
Figure 3.247: Load wedge-wedge expansion response of Test-75	170
Figure 3.248: Load wedge-wedge expansion response of Test-50	171
Figure 3.249: The average of load wedge-wedge expansion response of Test-125.....	171
Figure 3.250: Stress-wedge expansion response of Test-125.....	172
Figure 3.251: Stress-wedge expansion response of Test-100.....	173
Figure 3.252: Stress-wedge expansion response of Test-75.....	173
Figure 3.253: Stress-wedge expansion response of Test-50.....	174
Figure 3.254: The average of stress wedge-wedge expansion graph.....	174
Figure 3.255: The average of stress wedge-slip wedge graph.....	177
Figure 3.256: Non-dimensionalised stress-slip wedge.....	178
Figure 3.257: Slip wedge at peak stress over depth of wedge graph.....	179
Figure 3.258: Stress-slip comparison response of Test-125	179
Figure 3.259: Stress-slip comparison response of Test-100	180
Figure 3.260: Stress-slip comparison response of Test-75	180
Figure 3.261: Stress-slip comparison response of Test-50	181
Figure 3.262: The average of stress-wedge expansion graph.....	182
Figure 3.263: Non-dimensionalised stress-wedge expansion.....	182
Figure 3.264: Wedge expansion at peak stress over depth of wedge graph.....	183
Figure 3.265: Stress-wedge expansion comparison response of Test-125.....	183
Figure 3.266: Stress-wedge expansion comparison response of Test-100.....	184
Figure 3.267: Stress-wedge expansion comparison response of Test-75.....	184
Figure 3.268: Stress-wedge expansion comparison response of Test-50.....	184
Figure 4.1: Concrete and mortar cylinders test set up.	188
Figure 4.2: (a) Agregate compression test set up; (b) The diagram of transducers and strain gauges layout of aggregate	189
Figure 4.3: Layout of the transducers and strain gauges of concrete prism.	193
Figure 4.4: Concrete prism test set up; (a) side view (b) front view (face prism); (c) top view	194
Figure 4.5: Total axial load – contraction response of prism Test (II)1-125×375×500.....	195
Figure 4.6: Total axial load-dilation response of the prism Test (II)1-125×375×500	195

Figure 4.7:	Failure mode of concrete Test (II)1-125×375×500.....	196
Figure 4.8:	Total axial load – contraction response of the prism Test (II)2-125×375×500.	197
Figure 4.9:	Total axial load-dilation response of the prism Test (II)2-125×375×500	197
Figure 4.10:	Failure mode of concrete Test (II)2-125×375×500.....	198
Figure 4.11:	Total axial load - contraction response of the prism Test (II)3-125×375×500..	198
Figure 4.12:	Total axial load-dilation response of the prism Test (II)3-125×375×500	199
Figure 4.13:	Failure mode of concrete Test (II)3-125×375×500.....	199
Figure 4.14:	Total axial load - contraction response of the prism Test (II)4-125×250×500..	200
Figure 4.15:	Total axial load-dilation response of the prism Test (II)4-125×250×500	201
Figure 4.16:	Failure mode of concrete Test (II)4-125×250×500.....	201
Figure 4.17:	Total axial load-contraction response of the prism Test (II)5-125×250×500	202
Figure 4.18:	Total axial load-dilation response of the prism Test (II)5-125×250×500	202
Figure 4.19:	Failure mode of concrete Test (II)5-125×250×500.....	203
Figure 4.20:	Total axial load - contraction response of the prism Test (II)6-125×250×500..	203
Figure 4.21:	Total axial load-dilation response of the prism Test (II)6-125×250×500	204
Figure 4.22:	Failure mode of concrete test Test(II)6-125×250×500	204
Figure 4.23:	Total axial load - contraction response of the prism Test (II)7-125×125×500..	205
Figure 4.24:	Total axial load-dilation response of the prism Test (II)7-125×125×500	205
Figure 4.25:	Failure mode of concrete Test (II)7-125×125×500.....	206
Figure 4.26:	Total axial load - contraction response of the prism Test (II)8-125×125×500..	206
Figure 4.27:	Total axial load-dilation response of the prism Test (II)8-125×125×500	207
Figure 4.28:	Failure mode of concrete Test (II)8-125×125×500.....	207
Figure 4.29:	Total axial load - contraction response of the prism Test (II)9-125×125×500..	208
Figure 4.30:	Total axial load-dilation response of the prism Test (II)9-125×125×500	209
Figure 4.31:	Failure mode of concrete Test (II)9-125×125×500.....	209
Figure 4.32:	Total axial load - contraction response of the prism Test (II)10-100×200×400	210
Figure 4.33:	Total axial load-dilation response of the prism Test (II)10-100×200×400	210
Figure 4.34:	Failure mode of concrete (II)10-100×200×400.....	211
Figure 4.35:	Total axial load - contraction response of the prism Test (II)11-100×200×400	211
Figure 4.36:	Total axial load-dilation response of the prism Test (II)11-100×200×400	212
Figure 4.37:	Failure mode of concrete prism Test(II)11-100×200×400	212

Figure 4.38: Total axial load - contraction response of the prism (II)12-100×200×400	213
Figure 4.39: Total axial load-dilation response of the prism Test (II)12-100×200×400	213
Figure 4.40: Failure mode of concrete prism Test(II)12-100×200×400	214
Figure 4.41: Total axial load - contraction response of the prism (II)13-75×150×300	214
Figure 4.42: Total axial load-dilation response of the prism Test (II)13-75×150×300	215
Figure 4.43: Failure mode of concrete Test (II)13-75×150×300	215
Figure 4.44: Total axial load - contraction response of the prism Test(II)14-75×150×300 ...	216
Figure 4.45: Total axial load-dilation response of the prism Test (II)14-75×150×300	216
Figure 4.46: Failure mode of concrete Test (II)14-75×150×300	217
Figure 4.47: Total axial load - contraction response of the prism (II)15-75×150×300	217
Figure 4.48: Total axial load-dilation response of the prism Test (II)15-75×150×300	218
Figure 4.49: Failure mode of concrete Test (II)15-75×150×300	218
Figure 4.50: Total axial load - contraction response of the prism (II)16-50×100×200	219
Figure 4.51: Total axial load-dilation response of the prism Test (II)16-50×100×200	219
Figure 4.52: Failure mode of concrete Test (II)16-50×100×200	220
Figure 4.53: Total axial load - contraction response of the prism Test(II)17-50×100×200 ...	220
Figure 4.54: Total axial load-dilation response of the prism Test (II)17-50×100×200	221
Figure 4.55: Failure mode of concrete Test (II)17-50×100×200	221
Figure 4.56: Total axial load - contraction response of the prism (II)18-50×100×200	222
Figure 4.57: Total axial load-dilation response of the prism Test (II)18-50×100×200	223
Figure 4.58: Failure mode of concrete Test (II)18-50×100×200; (a) and (b) face/front view; (c) side view.....	223
Figure 4.59: Total axial load-total axial contraction for Test (II)1-125×375×500.....	225
Figure 4.60: Total axial load-total axial contraction for Test (II)1-125×375×500 (new axis)225	
Figure 4.61: Axial load-C/2 response of the prism Test (II)1-125×375×500	226
Figure 4.62: Axial load-slip wedge response of the prism Test (II)1-125×375×500.....	226
Figure 4.63: Load wedge-slip wedge response of the prism Test (II)1-125×375×500	227
Figure 4.64: The stress wedge-slip wedge response of the prism Test (II)1-125×375×500 ..	228
Figure 4.65: Total axial load–average dilation response of the prism Test (II)1-125×375×500	228

Figure 4.66: Total axial load-total lateral expansion response of the prism Test (II)1-125×375×500.....	229
Figure 4.67: Axial load – E/2 response of the prism Test (II)1-125×375×500.....	229
Figure 4.68: Axial load-wedge expansion response of the prism Test (II)1-125×375×500...	230
Figure 4.69: Load wedge-wedge expansion response of the prism Test (II)1-125×375×500	230
Figure 4.70: The stress wedge - wedge expansion response of the prism Test (II)1-125×375×500.....	231
Figure 4.71: Total axial load-total axial contraction response of the prism Test(II)-125×375×500.....	231
Figure 4.72: Axial load-C/2 response of the prism Test(II)-125×375×500	232
Figure 4.73: Axial load-slip wedge response of the prism Test(II)-125×375×500	233
Figure 4.74: Load wedge-slip wedge response of the prism Test(II)-125×375×500	233
Figure 4.75: Stress wedge-slip wedge response of the prism Test(II)-125×375×500	234
Figure 4.76: Total axial load-total lateral expansion for Test(II)-125×375×500.....	235
Figure 4.77: Axial load – E/2 response of the prism Test(II)-125×375×500.....	235
Figure 4.78: Axial load – wedge expansion response of the prism Test(II)-125×375×500...	236
Figure 4.79: Load wedge – wedge expansion response of the prism Test(II)-125×375×500	236
Figure 4.80: Stress wedge-wedge expansion response of the prism Test(II)-125×375×500 .	237
Figure 4.81: Total axial load-total axial contraction response of the prism Test(II)-125×250×500.....	239
Figure 4.82: Axial load-C/2 response of the prism Test(II)-125×250×500	239
Figure 4.83: Axial load-slip wedge response of the prism Test(II)-125×250×500	240
Figure 4.84: Load wedge-slip wedge response of the prism Test(II)-125×250×500	240
Figure 4.85: Stress wedge-slip wedge response of the prism Test(II)-125×250×500	241
Figure 4.86: Total axial load-total lateral expansion for Test(II)-125×250×500.....	241
Figure 4.87: Axial load – E/2 response of the prism Test(II)-125×250×500.....	242
Figure 4.88: Axial load – wedge expansion response of the prism Test(II)-125×250×500...	242
Figure 4.89: Load wedge – wedge expansion response of the prism Test(II)-125×250×500	243
Figure 4.90: Stress wedge-wedge expansion response of the prism Test(II)-125×250×500 .	243
Figure 4.91: Total axial load-total axial contraction response of the prism Test(II)-125×125×500.....	245

Figure 4.92: Axial load-C/2 response of the prism Test(II)-125×125×500	245
Figure 4.93: Axial load-slip wedge response of the prism Test(II)-125×125×500.....	246
Figure 4.94: Load wedge-slip wedge response of the prism Test(II)-125×125×500.....	246
Figure 4.95: Stress wedge-slip wedge response of the prism Test(II)-125×125×500	247
Figure 4.96: Total axial load-total lateral expansion for Test(II)-125×125×500	247
Figure 4.97: Axial load – E/2 response of the prism Test(II)-125×125×500	248
Figure 4.98: Axial load – wedge expansion response of the prism Test(II)-125×125×500 ...	248
Figure 4.99: Load wedge – wedge expansion response of the prism Test(II)-125×125×500	249
Figure 4.100: Stress wedge-wedge expansion response of the prism Test(II)-125×125×500	249
Figure 4.101: Total axial load-total axial contraction response of the prism Test(II)- 100×200×400	251
Figure 4.102: Axial load-C/2 response of the prism Test(II)-100×200×400	251
Figure 4.103: Axial load-slip wedge response of the prism Test(II)-100×200×400	252
Figure 4.104: Load wedge-slip wedge response of the prism Test(II)-100×200×400	252
Figure 4.105: Stress wedge-slip wedge response of the prism Test(II)-100×200×400	253
Figure 4.106: Total axial load-total lateral expansion for Test(II)-100×200×400.....	253
Figure 4.107: Axial load – E/2 response of the prism Test(II)-100×200×400.....	254
Figure 4.108: Axial load – wedge expansion response of the prism Test(II)-100×200×400...	254
Figure 4.109: Load wedge – wedge expansion response of the prism Test(II)-100×200×400	255
Figure 4.110: Stress wedge-wedge expansion response of the prism Test(II)-100×200×400 .	255
Figure 4.111: Total axial load-total axial contraction response of the prism Test(II)-75×150×30	257
Figure 4.112: Axial load-C/2 response of the prism Test(II)-75×150×300	257
Figure 4.113: Axial load-slip wedge response of the prism Test(II)-75×150×300	258
Figure 4.114: Load wedge-slip wedge response of the prism Test(II)-75×150×300	258
Figure 4.115: Stress wedge-slip wedge response of the prism Test(II)-75×150×300	258
Figure 4.116: Total axial load-total lateral expansion for Test(II)-75×150×300.....	259
Figure 4.117: Axial load – E/2 response of the prism Test(II)-75×150×300.....	259
Figure 4.118: Axial load – wedge expansion response of the prism Test(II)-75×150×300.....	260
Figure 4.119: Load wedge – wedge expansion response of the prism Test(II)-75×150×300..	260

Figure 4.120: Stress wedge-wedge expansion response of the prism Test(II)-75×150×300...	261
Figure 4.121: Total axial load-total axial contraction response of the prism Test(II)-50×100×200.....	262
Figure 4.122: Axial load-C/2 response of the prism Test(II)-50×100×200.....	262
Figure 4.123: Axial load-slip wedge response of the prism Test(II)-50×100×200.....	263
Figure 4.124: Load wedge-slip wedge response of the prism Test(II)-50×100×200.....	263
Figure 4.125: Stress wedge-slip wedge response of the prism Test(II)-50×100×200.....	264
Figure 4.126: Total axial load-total lateral expansion for Test(II)-50×100×200.....	264
Figure 4.127: Axial load – E/2 response of the prism Test(II)-50×100×200.....	265
Figure 4.128: Axial load – wedge expansion response of the prism Test(II)-50×100×200.....	265
Figure 4.129: Load wedge – wedge expansion response of the prism Test(II)-50×100×200..	266
Figure 4.130: Stress wedge-wedge expansion response of the prism Test(II)-50×100×200...	266
Figure 4.131: The average of total axial load-total axial contraction graph of Test (II) A.....	268
Figure 4.132: The average of total axial load-total axial contraction graph of Test (II) B.....	269
Figure 4.133: The average of axial load-C/2 graph of Test (II) A.....	270
Figure 4.134: The average of axial load-C/2 graph of Test (II) B.....	270
Figure 4.135: The average of axial load-slip wedge graph of Test (II) A.....	271
Figure 4.136: The average of axial load-slip wedge graph of Test (II) B.....	272
Figure 4.137: The average of load wedge-slip wedge graph of Test (II) A.....	272
Figure 4.138: The average of load wedge-slip wedge graph of Test (II) B.....	273
Figure 4.139: The average of stress wedge-slip wedge graph of Test (II) A.....	274
Figure 4.140: The average of stress-slip wedge graph of Test (II) B.....	274
Figure 4.141: Relative strength-height of prism graph.....	275
Figure 4.142: The average of L-E graph of Test(II) A.....	276
Figure 4.143: The average of L-E graph of Test (II) B.....	277
Figure 4.144: The average of axial load – E/2 graph of Test (II) A.....	278
Figure 4.145: The average of axial load – E/2 graph of Test (II) B.....	278
Figure 4.146: The average of axial load – wedge expansion graph of Test (II) A.....	279
Figure 4.147: The average of axial load – wedge expansion graph of Test (II) B.....	279
Figure 4.148: The average of load wedge – wedge expansion graph of Test (II) A.....	280
Figure 4.149: The average of load wedge – wedge expansion graph of Test (II) B.....	281

Figure 4.150: The average of stress wedge-wedge expansion graph of Test (II) A	282
Figure 4.151: The average of stress wedge-wedge expansion graph of Test (II) B	282
Figure 4.152: The stress-slip wedge of different size of prism-Test(II)A	284
Figure 4.153: Non-dimensionalised stress wedge-slip wedge of Test (II) A.....	284
Figure 4.154: Slip wedge at peak stress wedge over depth of wedge graph of TEST (II) A ...	285
Figure 4.155: Stress-slip comparison response of Test(II)-50×100×200.....	286
Figure 4.156: Stress-slip comparison response of Test(II)-75×150×300.....	286
Figure 4.157: Stress-slip comparison response of Test(II)-100×200×400.....	286
Figure 4.158: Stress-slip comparison response of Test(II)-125×250×500.....	287
Figure 4.159: The stress-slip wedge of different slenderness ratio of prism-Test(II)B	287
Figure 4.160: Non-dimensionalised stress-slip wedge of Test (II) B	288
Figure 4.161: The stress-slip comparison response of Test(II)-125×125×500.....	289
Figure 4.162: The stress-slip comparison response of Test(II)-125×250×500.....	289
Figure 4.163: The stress-slip comparison response of Test(II)-125×375×500.....	290
Figure 4.164: The average of stress-wedge expansion graph of Test (II) A	291
Figure 4.165: Non-dimensionalised stress-wedge expansion of Test (II) A.....	292
Figure 4.166: Wedge expansion at peak stress over depth of wedge graph [Test(II)A]	292
Figure 4.167: Stress-expansion comparison response of Test(II)-50×100×200.....	293
Figure 4.168: Stress-expansion comparison response of the prism Test(II)-75×150×300	293
Figure 4.169: Stress-expansion comparison response of the prism Test(II)-100×200×400	294
Figure 4.170: Stress-expansion comparison response of the prism Test (II)-125×250×500 ...	294
Figure 4.171: The average of stress-wedge expansion graph of Test (II) B	295
Figure 4.172: Non-dimensionalised stress-wedge expansion of Test (II) B	295
Figure 4.173: The stress-wedge expansion comparison response of Test(II)-125×125×500 ..	296
Figure 4.174: The stress-wedge expansion comparison response of Test(II)-125×250×500 ..	296
Figure 4.175: The stress-wedge expansion comparison response of Test(II)-125×375×500 ..	296
Figure 5.1: The wedge in millimeter thickness.....	300
Figure 5.2: The stress - slip wedge response	301
Figure 5.3: Eccentrically loaded prism	302
Figure 5.4: Graphic representation of an eccentrically loaded prism	302
Figure 5.5: Moment rotation analysis in elastic deformation.....	306

Figure 5.6:	The relationship between $P-C/2$ and σ_w-S_w of prism Test5-100.....	307
Figure 5.7:	Moment rotation analysis in the non-elastic deformation.....	311
Figure 5.8:	The segment n in the non-linear compressive region.....	311
Figure 5.9:	Moment Rotation for $f_p = 43\text{MPa}$, $e = 70\text{mm}$	312
Figure 5.10:	A typical the moment rotation response	313
Figure 5.11:	Moment - Non-linear rotation for $f_p = 43\text{MPa}$, $e = 70\text{mm}$	313
Figure 5.12:	Specimen dimension of Daniell's specimen [Daniell et al., 2008].....	314
Figure 5.13:	A typical moment-rotation comparison	314
Figure 5.14:	Moment-non-linear rotation for $e = 60\text{mm}$	315
Figure 5.15:	Moment-non-linear rotation for $e = 70\text{mm}$	316
Figure 5.16:	Moment-non-linear rotation for $e = 85\text{mm}$	316
Figure 5.17:	A typical of moment-curvature response.....	317



TABLE OF TABLES

Table 3.1: Material properties of 100mm×200mm concrete cylinders	24
Table 3.2: Material properties of five mortar cylinders.....	26
Table 3.3: Material properties of core aggregate cylinders.....	28
Table 3.4: Detail of concrete prism.....	32
Table 3.5: The important parameters of prism Test-125 based on individual graph	95
Table 3.6: The important parameters of prism Test-100 based on individual graph	113
Table 3.7: The important parameters of prism Test-75 based on individual graph	131
Table 3.8: The important parameters of prism Test-50 based on individual graph	143
Table 3.9: The average of important parameters of all concrete prism based on average curves	175
Table 4.1: Material properties of concrete	190
Table 4.2: Material properties of Mortar.....	190
Table 4.3: Material properties of aggregate	191
Table 4.4: Detail of concrete block	192
Table 4.5: The important parameters of prism Test(II)-125×375×500 based on individual graph	237
Table 4.6: The important parameters of prism Test(II)-125×250×500 based on individual graph	244
Table 4.7: The important parameters of prism Test(II)-125×125×500 based on individual graph	250
Table 4.8: The important parameters of prism Test(II)-100×200×400 based on individual graph	256
Table 4.9: The important parameters of prism Test(II)-75×150×300 based on individual graph	261
Table 4.10: The important parameters of prism Test(II)-50×100×200 based on individual graph	266
Table 4.11: Average of the peak value of concrete prism based on average curves (TEST II)	269

